

**Fig. 1.** Identification of T-DNA mutants that interrupt *EBF1* and -2. (A) Gene structures of *EBF1* and -2. Introns are indicated by lines. Shaded and white boxes indicate coding regions and 5' and 3' untranslated regions, respectively. The positions of the T-DNAs and the locations of the primers pairs used for RT-PCR are indicated. (B) RT-PCR analysis of the *EBF1* and -2 T-DNA insertion mutants. Total seedling RNA was reverse transcribed (RT) with either primer 2 or 4. The RT products were then PCR amplified. The A (primers 1 and 4) and C (primers 3 and 4) reactions used the first strand synthesis products from primer 4 whereas the B (primers 1 and 2) reactions used the first strand products created with primer 2. RT-PCR of *PAE2* was included as a control. (C) Gel blot analysis of *EBF1* and -2 mRNA. Total RNA from 11-day-old seedlings from the wild-type WS or Col-0 parents and the four T-DNA mutants was subjected to RNA gel blotting by using the *EBF1*, *EBF2*, and  $\beta$ -tubulin-4 (*TUB4*) sequences as probes.

by alterations in its half-life. Whereas ethylene appears to promote EIN3 stability, glucose, which antagonizes ethylene action, promotes its breakdown. This breakdown is dramatically retarded by the 26S proteasome-inhibitor MG132, suggesting that EIN3 levels are controlled by the Ub/26S proteasome pathway (13). Taken together, it appears that various signals, including ethylene, converge to directly modulate EIN3 turnover, possibly by inhibiting or promoting its ubiquitination by one or more E3s and/or subsequent turnover by the 26S proteasome.

In our attempts to functionally characterize the SCF E3 family in *Arabidopsis*, we initiated the reverse genetic analysis of a pair of F-box proteins related to yeast Grr1p, a leucine-rich repeat (LRR) F-box protein involved in glucose signaling and the cell cycle (14). Here, we show through phenotypic analyses that EIN3-binding F-box (EBF) 1 and 2 play an important role in regulating ethylene action and plant growth. Both the *EBF1* and -2 proteins interact directly with EIN3, and the loss of either enhances EIN3 accumulation *in vivo*, suggesting that these F-box proteins function in SCF complexes (SCF<sup>EBF1/2</sup>) that target EIN3 for ubiquitination and subsequent degradation. We also found that *ebf1 ebf2* double mutants display a severe growth inhibition after germination and have heightened levels of EIN3 even in the absence of exogenous ethylene, suggesting that EIN3 acts a general repressor of plant growth.

## Materials and Methods

**Alignments and Sequence Analysis.** Intron/exon organizations of *EBF1* and -2 were determined by comparing the genomic sequences with those from the cDNAs 118L22T7 (*EBF1*) and G1A5T7 (*EBF2*). Amino acid sequences were aligned by using CLUSTALX MAC V.1.6b (15) and displayed by MACBOXSHADE V.2.11 (Institute of Animal Health, Pirbright, UK). Yeast-two-hybrid (Y2H) was performed as described (3) by using the Clontech Matchmaker System (Palo Alto, CA).

**T-DNA Insertion Mutants.** The *ebf1-4* and *ebf2-4* T-DNA insertion lines were identified by PCR in the University of Wisconsin, Madison T-DNA-transformed population of *Arabidopsis* ecotype Wassilewskija (WS) ([www.biotech.wisc.edu/Arabidopsis](http://www.biotech.wisc.edu/Arabidopsis)) using 5' and 3' gene-specific primers in combination with T-DNA-specific primers. Both WS alleles were backcrossed three times to wild-type *Arabidopsis* WS. The *ebf1-3* (SALK-020997) and *ebf2-3* (SALK-092571) T-DNA insertion lines were identified in the SIGNAL T-DNA collection (<http://signal.salk.edu/cgi-bin/tdnaexpress>) generated from the Col-0 ecotype and obtained from the *Arabidopsis* Biological Resource Center (Columbus, OH).

**RNA Isolations, RNA Gel Blot Analysis, and RT-PCR.** Total seedling RNA was isolated and subjected to RNA-gel blot analysis according to Smalle *et al.* (16). <sup>32</sup>P-labeled riboprobes were synthesized by using the appropriate linearized plasmids and the Riboprobe Gemini II core system (Promega). The  $\beta$ -*TUB4* and *RPN3a* templates were as described (17). The *b-CHI* and *EBP* templates used the EST clones 92G1 and 166N3 ([www.arabidopsis.org](http://www.arabidopsis.org)), respectively. The *EBF1* and -2 templates were made by amplifying the full-length cDNAs and inserting them into pGEM-T plasmids (Promega).

For RT-PCR, each first-strand cDNA reaction was performed by using an *EBF1*- or -2-specific primer (primer 2 or 4), a *PAE2*-specific primer, 1  $\mu$ g of RNA, and Moloney murine leukemia virus RTase (Promega). Primers for *EBF1* are as follows: 1, TTCCTGGAGTTTTGAGCTCA; 2, CAGCCCCGACACCATTCCAT; 3, GTTGAAGGCTTCTCTCTGGT; 4, GTTGATCAGGAGAGGATGTCA. Primers for *EBF2* are as follows: 1, GTCTGGAATCTTCAGATTTAGTG; 2, CCTTTACCAGAAACAAGCAAGCA; 3, ACTTTGGTCTCAGATCACGGA; 4, AGACTTGGACTGATGATGATGA. The position of each is identified left to right in Fig. 1. The *PAE2* primers are as described (18).

**Phenotypic Analyses.** Unless otherwise noted, plants were grown on Gamborg's B5 growth medium (GM) (Gibco BRL) at 21°C under a long-day photoperiod (16 h light/8 h dark) after a 4-day stratification at 4°C. For hypocotyl growth measurements of ACC-treated seedlings, seed was plated on 1/2 $\times$  MS medium containing 1% sucrose and various concentrations of ACC, exposed to 1.5 h of white light after stratification, and grown horizontally in the dark at 24°C for 5.5 days. For hypocotyl measurements of ethylene-treated seedlings, the seed was plated on 1/2 $\times$  MS medium containing 5  $\mu$ M aminoethoxyvinylglycine (AVG), exposed to white light for 3 h after stratification, and grown vertically in the dark for 3.5 days at 24°C with or without exposure to ethylene. Root growth measurements were done by transferring 5-day-old seedlings of equal size to 1/2 $\times$  MS medium containing 1% sucrose and various concentrations of ACC and growing them vertically for an additional 5 days. For the immunoblot analysis, seedlings were exposed to air or ethylene, frozen to liquid nitrogen temperature, and homogenized directly into SDS/PAGE sample buffer. The clarified extracts were subjected to SDS/PAGE and immunoblot analysis according to (16). Antibodies against EIN3, PBA1, and Ub were prepared as described (13, 16).

## Results

To help define the functions and targets for the numerous SCF E3s in *Arabidopsis* (3), we initiated the reverse genetic analysis of

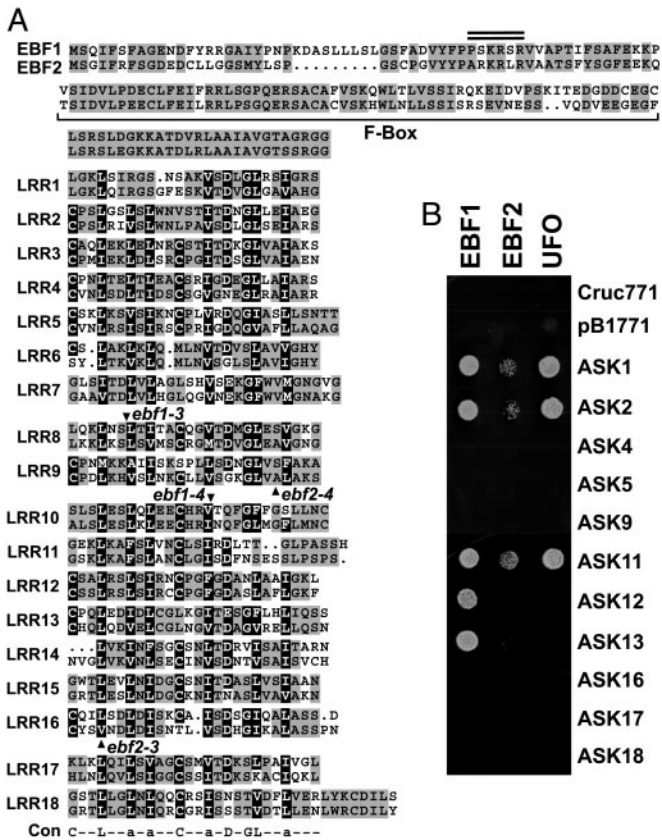


**Fig. 2.** EBF1 and -2 are F-box proteins. (A) Amino acid sequence alignment of EBF1 and -2. The F-box motif and the potential NLS are defined by the bracket and the double line, respectively. Gray shading indicates residues that are similar or identical between EBF1 and -2. The 18 LRR-CCs are aligned with the consensus sequence (Con) (a = aliphatic). The black shading denotes similarities among the 18 LRRs. The black shading denotes similarities among the 18 LRRs. Arrowheads mark T-DNA insertion sites. (B) Y2H analysis of the interactions between EBF1 and -2 and representative ASKs. Yeast strains were grown at 28°C for 4 days on 10 mM 3-AT. Empty vectors (pB1771 and pB1770) or vectors expressing cruciferin (Cruc771 and Cruc770) or the F-box protein UFO were included as controls.

representative members of the F-box protein family. EBF1 (At2g25490) and -2 (At5g25350) were selected because of their similarity to Grr1p (33%), a well-characterized yeast F-box protein involved in sugar signaling and cell division (14, 19). EBF1 and -2 encode 628- and 623-amino acid proteins, respectively, and are members of the C4 subfamily (3). Both proteins have a predicted nuclear localization sequence (NLS) near the N terminus, followed by a ≈61-residue F-box motif, and terminate in 18 cysteine-containing (CC) LRRs (Fig. 2A). Potential orthologs of EBF1 and -2 were detected in a variety of other plant species, including similarly duplicated loci in rice, soybean, and *Medicago truncatula* (data not shown). The *Arabidopsis* loci are in blocks of weak synteny potentially duplicated after the monocot/dicot split (20), suggesting that the EBF1/2 subfamily predates crucifer speciation.

Although related in sequence to yeast Grr1p, EBF1 or -2 were unable to functionally replace the yeast F-box protein. Expression of either *Arabidopsis* protein in the *grr1Δ* mutant failed to rescue any of its mutant phenotypes (14), including the elongated cell growth, hypersensitivity to nitrogen starvation and osmotic stress, and a slow growth on media containing glucose or raffinose (data not shown). Proof that EBF1 and -2 can assemble into SCF complexes was provided by Y2H analysis, which showed that both proteins interact with one or more *Arabidopsis* Skps (ASKs). By using both 3-amino-1,2,4-triazole (3-AT) resistance and β-galactosidase activ-

ity for the assays, we observed interactions between EBF1 and -2 and several representative ASKs (Fig. 2B and data not shown).

EBF1 and -2 are highly similar to each other (57/75% identity/similarity) relative to other *Arabidopsis* F-box proteins (3), suggesting that they have related functions/targets. To further characterize the roles of EBF1 and -2 in *planta*, we phenotypically analyzed T-DNA insertion lines disrupting the corresponding genes in the Col-0 and WS ecotypes. All four mutants contain a T-DNA within the second exon and thus should alter target recognition by the LRR-CC domain of the resulting proteins if expressed (Figs. 1A and 2A). For *ebf1-3* (Col-0), the T-DNA inserted after codon 339 (bp 1388) and generated a deletion of bp 1389–1401. For *ebf1-4* (WS), the T-DNA interrupted the 400th codon (bp 1570) and generated a deletion of bp 1571–1576. For *ebf2-3* (Col-0) and *ebf2-4* (WS) the T-DNA inserted in codon 540 (bp 1787) and codon 371 (bp 1280), respectively.

RT-PCR amplification of EBF1 and -2 transcripts revealed that all four T-DNA insertions interfere with the production of wild-type mRNAs. As can be seen in Fig. 1B, partial transcripts could be amplified for regions 5' and/or 3' to the T-DNA inserts, but no complete transcript spanning the inserts could be amplified. The 5' transcripts were probably initiated naturally from the EBF1 and -2 promoters (B products), whereas the 3' transcripts (C products) were likely generated artifactually by known promoter elements present within the T-DNAs (pROK2 and pSKI1015). Gel blot analysis further confirmed that the mutant lines do not accumulate normal EBF1 and 2 mRNAs (Fig. 1C). Truncated mRNAs were evident in the *ebf1-3*, *ebf1-4*, and *ebf2-4* lines. For the *ebf2-3* line, an mRNA similar in size to the wild-type EBF2 transcript (≈2.6 Kb) was detected. However, subsequent sequence analysis revealed that this *ebf2-3* transcript was a chimeric mRNA in which the codons for the 83 C-terminal amino acids and the 3' UTR were replaced by similar length of T-DNA sequence.

*Arabidopsis* plants homozygous for *ebf1* or *ebf2* mutations germinated, grew, flowered, and set seeds similar to wild type under normal growth conditions, indicating that neither F-box protein is essential on its own (Fig. 3A and B and data not shown). The only visible change was a slight decrease in root growth for the *ebf1-3* and *ebf1-4* seedlings. To search for conditional phenotypes, we grew the homozygous mutants under a variety of adverse growth conditions and in the presence of various growth regulators. A marked hypersensitivity was seen for the *ebf2-3* and *ebf2-4* seedlings when exposed to the ethylene precursor ACC. As shown in Fig. 3B, root growth for the *ebf2* mutants was more inhibited by ACC than the wild-type controls, whereas the roots of the *ebf1* mutants were shorter with or without ACC. Additionally, the *ebf2* mutants exhibited a dramatic increase in root hair length on only 0.05 μM ACC, whereas wild-type or *ebf1* roots needed a much higher ACC concentration to elicit the same effect (Fig. 3C). Both root phenotypes are similar to those found in mutants with enhanced ethylene responses (10), suggesting that the EBF2 protein (and possibly EBF1) is a repressor of ethylene action.

To further characterize their increased sensitivity to ethylene, we examined dark grown *ebf1* and -2 seedlings exposed to ACC or ethylene. For the experiments using ethylene, the seedlings were also treated with the ethylene biosynthesis inhibitor aminoethoxyvinylglycine (AVG), which effectively represses endogenous production of the hormone. Both ethylene and ACC induce the triple response, part of which is an inhibition of hypocotyl growth (10). The *ebf2* seedlings showed a greater inhibition of hypocotyl growth than the *ebf1* or wild-type seedlings when treated with 0.2 μM ACC (Fig. 4A). When treated with ethylene and AVG, the *ebf2* lines displayed an increased capacity to respond. Specifically, the *ebf2-3* and *ebf2-4* mutants responded near normal to low concentrations of ethylene but displayed a dramatic response at saturating concentrations (≥150 ppm), including extremely short and swollen hypocotyls and little or no root growth (Fig. 4B and C and data not shown). This phenotype was even more severe than that observed

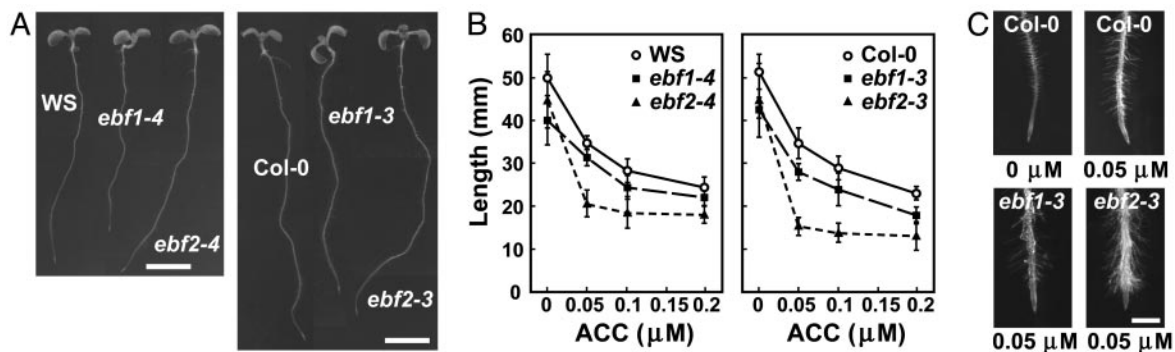


**Fig. 3.** T-DNA disruptions in *EBF1* and *-2* alter sensitivity of roots to ACC. (A) Six-day-old wild-type and mutant seedlings grown under a long-day photoperiod. Scale bar = 5 mm. (B) Root growth of seedlings grown for 5 days without ACC and then transferred to medium containing various concentrations of ACC and grown for an additional 5 days. Each point represents the average ( $\pm$  SD) of 12 seedlings. (C) Representative root tips from Col-0, *ebf1-3*, and *ebf2-3* individuals grown on medium without or with 0.05  $\mu$ M ACC. Scale bar = 1 mm.

for the constitutive ethylene-response mutant *ctr1-4* when exposed to supersaturating concentrations of ethylene, suggesting a strong increase in ethylene responsiveness. In contrast, the *ebf1* seedlings

showed a weak constitutive response to ethylene. In the presence of AVG and low or no concentrations of ethylene, hypocotyl elongation of the *ebf1-3* and *ebf1-4* lines was significantly reduced when compared to wild type (Fig. 4B and C and data not shown). At high ethylene concentrations, this difference was eliminated.

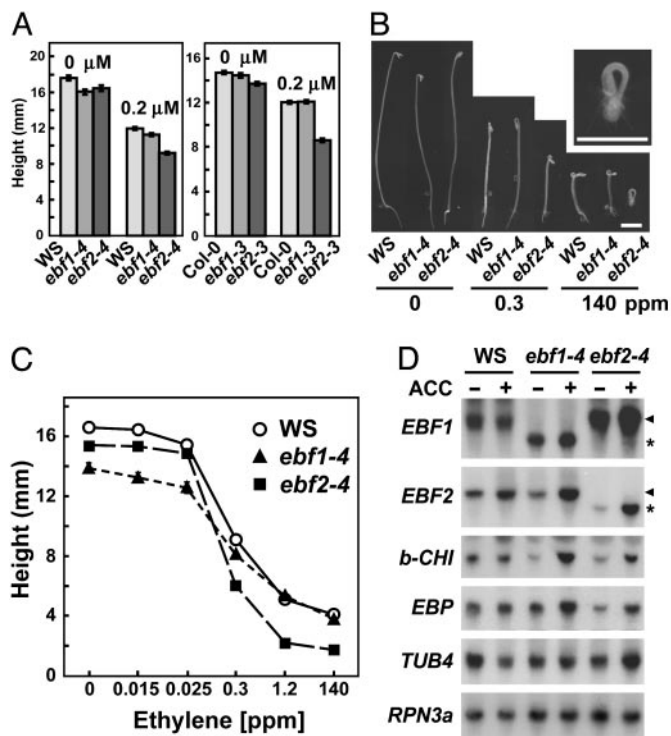


**Fig. 4.** T-DNA disruptions of *EBF1* and *-2* alter the sensitivity of etiolated shoots to ACC and ethylene. (A) Hypocotyl elongation of etiolated seedlings grown for 5.5 days on medium without or with 0.2  $\mu$ M ACC. Each bar represents the average of 50 seedlings ( $\pm$  SEM). (B and C) Hypocotyl elongation of etiolated WS, *ebf1-4*, and *ebf2-4* seedlings treated for 3.5 days with various concentrations of ethylene. (B) Representative seedlings of each genotype after treatment with 0, 0.3, and 140 ppm ethylene (Scale bar = 2 mm). A magnification of an *ebf2-4* seedling treated with 140-ppm ethylene is shown on the right. (C) Hypocotyl elongation of seedlings treated with various concentrations of ethylene. Each point represents the average of  $\geq$ 33 seedlings ( $\pm$  SEM). (D) Effect of the *ebf1-4* and *ebf2-4* mutations on ethylene-induced gene expression. Liquid culture-grown seedlings were treated for 4 h without or with 50  $\mu$ M ACC. Blots of total RNA were probed for *EBF1* and *-2* and the ethylene-inducible mRNAs, *b-CHI* and *EBP*. mRNAs for  $\beta$ -tubulin (*TUB4*) and the 26S proteasome subunit *RPN3a* were used as controls. The arrowheads and asterisks indicate the position of the wild-type *EBF1* and *-2* mRNAs and truncated *ebf1-4* and *ebf2-4* mRNAs, respectively.

Together these phenotypic data suggest that *EBF1* and *2* have roles in repressing ethylene action. To document this repression at the molecular level, we examined the expression patterns of *EBF1* and *-2* and several ethylene-inducible genes in *ebf1-4*, *ebf2-4*, and WS seedlings after a 4-hour exposure to 50  $\mu$ M ACC. The ACC treatment was suboptimal to allow the detection of hypersensitive responses. For example, the mRNAs of *EBP* and *b-CHI*, which are strongly increased after 12 h of exposure to 1 mM ACC (11), were not up-regulated in wild-type WS after this short treatment (Fig. 4D). However, an increase in both transcripts was evident in the *ebf1-4* and *ebf2-4* mutants, consistent with ethylene hypersensitivity. *EBF2* transcript levels also increased after ACC treatment. This increase, although evident in the wild-type seedlings, became more pronounced in the mutant backgrounds, indicating that ethylene positively regulates *EBF2* mRNA abundance via a mechanism that is repressed by both *EBF1* and *-2*. That suboptimal ACC treatment induced the accumulation of *EBF2* transcript but not *EBP* and *b-CHI* suggests that up-regulation of *EBF2* expression is an early response to ethylene perception.

The incorporation of *EBF1* and *-2* into SCF E3 complexes and the ethylene hypersensitivity of the corresponding mutants implied that these F-box proteins direct the ubiquitination and subsequent degradation of one or more positive regulators of ethylene action. One likely target was *EIN3*, whose levels are critical for appropriate ethylene actions (10). Previous studies showed that *EIN3* is not regulated transcriptionally (12), whereas more recent data indicates that *EIN3* is degraded in an ethylene- and glucose-sensitive mechanism by the 26S proteasome (13).

To test whether *EBF1* and *-2* target *EIN3* for degradation, we first examined whether *EIN3* directly interacts with these two F-box proteins by Y2H. *EIN3* interacted with both *EBF1* and *-2* using both 3-AT resistance and  $\beta$ -galactosidase activity assays (Fig. 5A and data not shown). Conversely, no interaction was seen between *EIN3* and another F-box protein, *UFO*, indicating that the interaction was specific. We next determined whether the levels of *EIN3* are elevated in the *ebf1* and *ebf2* mutants. Here, *EIN3* protein was measured immunologically in seedlings with or without exposure to ethylene. As can be seen in Fig. 5B, we detected *EIN3* as a 78-kDa species that was present in wild-type but not *ein3-1* seedlings. Consistent with previous studies (13), *EIN3* was nearly undetectable in wild-type seedlings without ethylene treatment but rose dramatically after ethylene exposure. In *ebf1* and *ebf2* seedlings, the level of *EIN3* was increased in the absence of hormone (Fig. 5B).

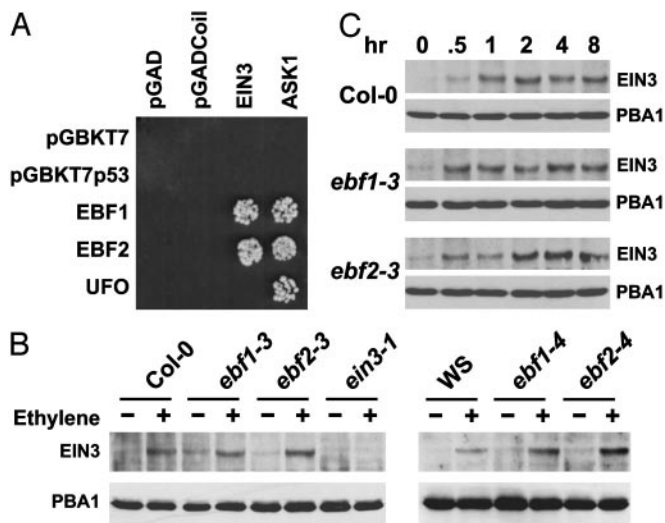


**Fig. 5.** Levels of EIN3 are increased in the *ebf1* and *ebf2* mutants. (A) Y2H analysis demonstrating the interactions of EBF1 and EBF2 with EIN3. Yeast strains were grown at 28°C for 3 days on 5 mM 3-AT. Empty vectors (pGAD and pGBKT7) or vectors expressing p53, the F-box protein UFO, or a coiled-coil domain protein were included as controls. Mutant seedlings and their respective wild-type parents (Col-0 and WS) were grown under a long-day photoperiod for 12 days and then treated for 4 h (B) or the indicated times (C) with 10 ppm ethylene. Equal amounts of crude extracts were subjected to SDS/PAGE and immunoblot analysis with anti-EIN3 and anti-PBA1 antibodies.

Time course studies indicated that both sets of *ebf1/2* mutants affected EIN3 turnover differentially (Fig. 5C and data not shown). In *ebf1* mutants, the ethylene induction was faster but reached the same level as wild type, whereas in the *ebf2* mutants, the kinetics of induction was similar to wild type but the final level of EIN3 was higher.

Given the likelihood that inactivation of both *EBF1* and *-2* further enhances EIN3 stability and thus ethylene sensitivity, we examined double homozygous *ebf1 ebf2* mutants. These mutants were generated by selfing plants homozygous for either *ebf1* or *ebf2* and heterozygous for the other locus. In both the WS and Col-0 backgrounds, a small population of severely defective progeny was detected after germination. They slowly emerged from the seed coat as dramatically stunted seedlings that failed to progress developmentally. Aberrant phenotypes included a severe inhibition of root and shoot growth, a dramatic increase in the number of root hairs, enhanced anthocyanin accumulation, accelerated senescence of the cotyledons, and a failure to develop true leaves, stems, and flowers (Fig. 6A and data not shown). The stunted seedlings remained at this juvenile stage for many weeks. Surprisingly, the arrested plants from the WS background eventually developed slow-growing calli from the root and shoot apices, which could then be maintained indefinitely on hormone-free medium (Fig. 6A). Root hairs often emerged ectopically from these calli, suggesting that these dividing cell masses acquired a root-like identity.

We verified that the stunted plants for each cross were the expected *ebf1 ebf2* double mutants by genotyping individual seedlings generated from multiple independent selfed populations. For example, when progeny from plants homozygous for *ebf1-4* but heterozygous for *ebf2-4* were germinated, all 39 of the normal plants tested had at least one wild-type copy of *EBF2*, whereas all 22 of the stunted plants tested were homozygous for the *ebf2-4* allele. The percentage of the stunted plants in each selfed population was lower than expected, suggesting a reduced transmission of one or both gametes. Instead of the predicted 25% of the progeny being double homozygotes, we detected only 18% and 6% for the WS and Col-0 selfed populations, respectively. The Col-0 *ebf1-3 ebf2-3* seedlings

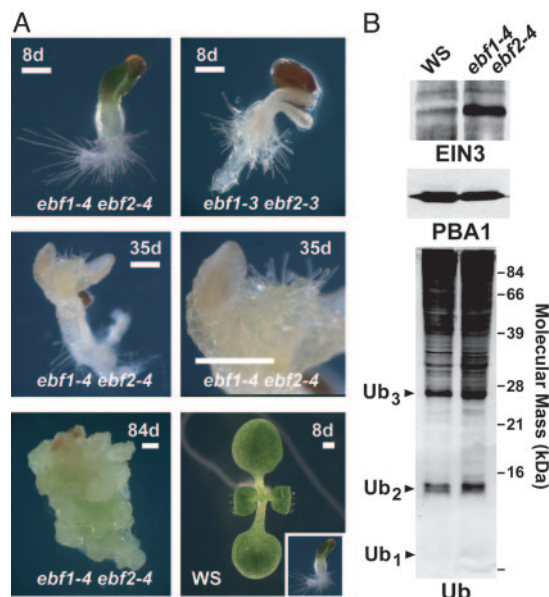


**Fig. 6.** Double homozygous mutants defective in both *EBF1* and *EBF2* display a severe growth arrest and enhanced EIN3 levels in the absence of ethylene. (A) Representative mutant and wild-type seedlings grown in a long-day photoperiod. The relative sizes of the 8-day-old wild-type and *ebf1-4 ebf2-4* seedlings are shown (*bottom right*). A higher magnification (*middle right*) illustrates the ectopic growth of root hairs from calli derived from the shoot meristem of *ebf1-4 ebf2-4* seedlings. Scale bar = 0.5 mm. (B) Levels of EIN3 and Ub conjugates in young *ebf1-4 ebf2-4* seedlings as compared to those in wild-type WS seedlings of a comparable developmental age. Equal amounts of crude extracts were subjected to SDS/PAGE and immunoblot analysis with antibodies against EIN3, PBA1, and Ub.

were also bleached, a phenotype seen less often in the WS double mutants (Fig. 6A), suggesting that this background is more sensitive to loss of this F-box protein pair. The growth inhibition for the double mutants in the absence of ethylene was more severe than that seen for the single *ebf2* mutants exposed to high concentrations of ethylene, suggesting that the phenotype of the double mutants reflected a very strong constitutive ethylene response (Figs. 4B and 6A).

We predicted that the double *ebf1 ebf2* mutants fail to degrade EIN3 and thus contain elevated EIN3 levels even without exogenous ethylene. To test this hypothesis, we hand picked double mutant seedlings based on the stunted phenotype from progeny of a selfed *ebf1-4/ebf1-4 ebf2-4/EBF2* plant and compared their EIN3 levels to that in wild-type WS seedlings collected at a similar developmental stage. As shown in Fig. 6B, the level of EIN3 was dramatically higher in the double mutant consistent with a strong stabilization of the protein. Similar analysis with anti-Ub antibodies showed loss of both F-box proteins did not appreciably alter the overall ubiquitination pattern and thus SCF<sup>EBF1/2</sup> may be EIN3-specific (Fig. 6).

## Discussion

Recent studies have implicated protein turnover by the Ub/26S proteasome in several aspects of ethylene synthesis and perception in plants (13). Our studies of *Arabidopsis EBF1* and *-2* show that this two-member F-box subfamily regulates ethylene signaling by targeting the EIN3 transcriptional regulator for degradation. Consistent with this proposal are our observations that (i) T-DNA insertion mutants for *EBF1* and/or *-2* display aberrant phenotypic and molecular responses to exogenous ethylene and its precursor ACC, (ii) both F-box proteins interact directly by Y2H with EIN3, (iii) ethylene-induced accumulation of EIN3 is enhanced in the *ebf1* and *-2* lines, and (iv) double homozygous *ebf1 ebf2* mutants display

a developmental phenotype predicted for plants hyperresponding to the hormone, including an extreme growth inhibition and ectopic production of root hairs. These results now add ethylene to the rapidly expanding list of plant hormones whose responses are directly regulated through the removal of a key activator/repressor by the Ub/26S proteasome pathway (1, 8, 9).

Why are two SCF complexes used to negatively regulate EIN3 levels? Collectively, the single and double mutant phenotypes of *ebf1* and *ebf2* seedlings suggest that the corresponding F-box proteins work synergistically to remove EIN3. For EBF1, the mutant phenotype is most evident at low ethylene concentrations, suggesting that the main function of the corresponding SCF<sup>EBF1</sup> complex is to constitutively target EIN3 for ubiquitination, thereby repressing the ethylene response at low hormone concentrations by keeping EIN3 below a critical threshold. The modest increase in EIN3 abundance seen in untreated *ebf1* mutants, the more rapid accumulation of EIN3 in ethylene-treated *ebf1* mutants, and the failure of ethylene to elevate *EBF1* mRNA abundance in wild-type seedlings support this early role. For EBF2, the phenotypic consequence of the mutations is most pronounced at saturating ethylene concentrations, suggesting a negative role for the corresponding SCF<sup>EBF2</sup> complex after the ethylene sensing pathway is engaged. In this capacity, EBF2 may act to repress prolonged ethylene responsiveness or dampen the signal by removing activated EIN3. The up-regulation of *EBF2* transcripts by ACC is consistent with the greater need for this F-box protein as ethylene levels rise. The concerted action of EBF1 and -2 may be essential to avoid excess accumulation of EIN3 throughout the life cycle of *Arabidopsis* given the strong inhibitory effect of this transcriptional regulator on seedling growth and development.

The combined importance of both EBF1 and -2 in ethylene action and plant growth is strikingly evident in the double *ebf1 ebf2* mutants. These individuals display a severe growth arrest after germination coupled with several accentuated ethylene-related phenotypes (10), including swollen hypocotyls and an inhibition of cotyledon expansion, ectopic emergence of root hairs, a strong anthocyanin accumulation, and accelerated senescence of the cotyledons. The developmental arrest may also reflect a substantial inhibition of cell division, which is supported by the ability of ethylene to arrest the cell cycle at the G2 phase (21). The growth arrest of the *ebf1 ebf2* mutants is much stronger than those previously observed for constitutive ethylene response mutants. For example, null alleles of *CTR1* resemble the wild type treated with saturating concentrations of ethylene (22), whereas a quadruple knockout of 4 of the 5 ethylene receptors generates a phenotype more severe than *ctr1-4* but weaker than what we observed for both *ebf1 ebf2* double mutants (23). That the *ebf1 ebf2* mutant phenotype is stronger than those of null *ctr1* mutants (22) is consistent with the corresponding SCF<sup>EBF1/EBF2</sup> E3s acting downstream of *CTR1*. In this model, these E3s would partially suppress the constitutive activation caused by loss of *CTR1* activity.

After completion of this work, Potushak *et al.* (24) and Guo and Ecker (25) reported a similar role for EBF1 and -2 in ethylene signaling and EIN3 degradation. In both cases, removal of EIN3 abolished the ethylene hypersensitive phenotype, further confirming EIN3 as a target of the SCF<sup>EBF1/EBF2</sup> complex. However, given that ethylene-hypersensitive phenotypes for individual mutants within their collections were sometimes milder than those observed here and that their double *ebf1 ebf2* mutants did not display a severe growth arrest, it is likely that some of the *ebf1* and *ebf2* alleles used were weaker than those studied here (24, 25).

Although we identified EIN3 as a target for the SCF<sup>EBF1/EBF2</sup> complexes, it is possible these E3s recognize other substrates as well. However, the similar profile of ubiquitinated proteins in the *ebf1-4 ebf2-4* double mutant seedlings relative to wild type suggests that this number is not large. One likely class of additional targets is the family of EIN3-related proteins (EILs) of which EIL1 is known to be involved in ethylene signaling (12, 24).

How EBF1/2 recognizes EIN3 is not yet clear. Many SCF E3s bind to their targets after signal-dependent phosphorylation of the target (2). For example, yeast Grr1p uses its LRR domain to bind to and ubiquitinate the phosphorylated forms of cyclins Cln1 and -2 (19). In a similar fashion, phosphorylation of EIN3 by the mitogen-activated protein kinase cascade directed by CTR1 may promote recognition by the LRR-CC domain in EBF1/2. Alternatively, the SCF<sup>EBF1/EBF2</sup> complex may be regulated by ethylene. For example, ethylene-induced modification of EBF1 and/or EBF2 could reduce their stability and/or affinity for EIN3, thus increasing the half-life of EIN3.

This study expands upon the recent work by Yanagisawa *et al.* (13), which showed via inhibitor studies that the 26S proteasome is important for regulating EIN3 abundance. Their study demonstrated that EIN3 turnover is enhanced by glucose, suggesting that additional signals impact EIN3 ubiquitination. As such, EIN3 may represent a more central suppressor of plant growth capable of integrating various external and internal signals. How glucose affects EIN3 turnover is not yet clear. It could involve recognition of EIN3 by SCF<sup>EBF1/EBF2</sup> or by another E3 yet to be discovered. However, a connection between SCF<sup>EBF1/EBF2</sup> and sugar is suggested by the sequence similarity of EBF1/2 to yeast Grr1p. In yeast, SCF<sup>Grr1</sup> acts downstream of hexokinase by derepressing several glucose-activated genes (14, 19). In a similar fashion, regulated degradation of EIN3 by SCF<sup>EBF1/EBF2</sup> may be affected by glucose in addition to ethylene. It is clear that discovering how ethylene and glucose direct the ubiquitination of EIN3 by SCF complexes like SCF<sup>EBF1/EBF2</sup> will be crucial to understand how these two signals converge to regulate plant development.

We thank Dr. Tony Bleeker and Dr. Brad Binder for help with the ethylene treatments and Dr. Jen Sheen for the anti-EIN3 antibodies. This work was supported by National Science Foundation (NSF) *Arabidopsis* 2010 Program Grant MCB-0115870 (to R.D.V.). S.-D.Y. was supported by NSF Plant Genome Program DBI-0077692, and D.J.G. was supported by a National Institutes of Health postdoctoral fellowship.

1. Smalle, J. & Vierstra, R. D. (2004) *Annu. Rev. Plant Biol.*, in press.
2. Deshaies, R. J. (1999) *Annu. Rev. Cell. Dev. Biol.* **15**, 435–467.
3. Gagne, J. M., Downes, B. P., Shiu, S. H., Durski, A. M. & Vierstra, R. D. (2002) *Proc. Nat. Acad. Sci. USA* **99**, 11519–11524.
4. Gray, W. M., Hellmann, H., Dharmasiri, S. & Estelle, M. (2002) *Plant Cell* **14**, 2137–2144.
5. Shen, W. H., Parmentier, Y., Hellmann, H., Lechner, E., Dong, A., Masson, J., Granier, F., Lepiniec, L., Estelle, M. & Genschik, P. (2002) *Mol. Biol. Cell.* **13**, 1916–1928.
6. Lechner, E., Xie, D. X., Grava, S., Pigaglio, E., Planchais, S., Murray, J. A. H., Parmentier, Y., Mutterer, J., Dubreucq, B., Shen, W. H. & Genschik, P. (2002) *J. Biol. Chem.* **277**, 50069–50080.
7. Yang, M., Hu, Y., Lodhi, M., McCombie, W. R. & Ma, H. (1999) *Proc. Natl. Acad. Sci. USA* **96**, 11416–11421.
8. Itoh, H., Matsuoka, M. & Steber, C. M. (2003) *Trends Plant Sci.* **8**, 492–497.
9. Hellmann, H. & Estelle, M. (2002) *Science* **297**, 793–797.
10. Schaller, G. E. & Kieber, J. J. (2002) in *The Arabidopsis Book*, eds Somerville, C. R. & Meyerowitz, E. M. (American Society of Plant Biologists, Rockville, MD), pp. 1–17.
11. Ouaked, F., Rozhon, W., Lecourieux, D. & Hirt, H. (2003) *EMBO J.* **22**, 1282–1288.
12. Solano, R., Stepanova, A., Chao, Q. M. & Ecker, J. R. (1998) *Genes Dev.* **12**, 3703–3714.
13. Yanagisawa, S., Yoo, S.-D. & Sheen, J. (2003) *Nature* **425**, 521–525.
14. Li, F. N. & Johnston, M. (1997) *EMBO J.* **16**, 5629–5638.
15. Thompson, J. D., Gibson, T. J., Plewniak, F., Jeanmougin, F. & Higgins, D. G. (1997) *Nucleic Acids Res.* **24**, 4876–4882.
16. Smalle, J., Kurepa, J., Yang, P., Babychuk, E., Kushnir, S., Durski, A. & Vierstra, R. D. (2002) *Plant Cell* **14**, 17–32.
17. Yang, P., Fu, H., Walker, J., Papa, C. M., Smalle, J., Ju, Y.-M. & Vierstra, R. D. (2004) *J. Biol. Chem.* **186**, 445–453.
18. Downes, B. P., Stupar, R. M., Gingerich, D. J. & Vierstra, R. D. (2003) *Plant J.* **35**, 729–742.
19. Hsiung, W. G., Chang, H. C., Pellequer, J. L., La Valle, R., Lanker, S. & Wittenberg, C. (2001) *Mol. Cell. Biol.* **21**, 2506–2520.
20. Blanc, G., Hokamp, K. & Wolfe, K. H. (2003) *Genome Res.* **13**, 137–144.
21. Dan, H., Imaseki, H., Wasteneys, G. O. & Kazama, H. (2003) *Plant Physiol.* **133**, 1726–1731.
22. Kieber, J. J., Rothenberg, M., Roman, G., Feldmann, K. A. & Ecker, J. R. (1993) *Cell* **12**, 427–441.
23. Hua, J. & Meyerowitz, E. M. (1998) *Cell* **94**, 261–271.
24. Potushak, T., Lechner, E., Parmentier, Y., Yanagisawa, S., Grava, S., Koncz, C. & Genschik, P. (2003) *Cell* **115**, 679–689.
25. Guo, H. W. & Ecker, J. R. (2003) *Cell* **115**, 667–677.